Energy 106 (2016) 137–146

Contents lists available at ScienceDirect

Energy

journal homepage: www.elsevier.com/locate/energy

New neural network and fuzzy logic controllers to monitor maximum power for wind energy conversion system

Ahmed Medjber [a, b], Abderrezak Guessoum [b], Hocine Belmili [c, *], Adel Mellit [d]

[a] LREA, Research Laboratory of Electronics and Automatics, University Yahia Fares, Médea, Algeria
[b] LATSI, Research Laboratory of Signal Processing and Imagery, Electronics Department, University Saad Dehleb, Blida, Algeria
[c] Unité de Développement des Equipements Solaires, UDES/Centre de Développement des Energies Renouvelables, CDER, Bou Ismail, 42415, W. Tipaza, Algeria
[d] Faculty of Sciences Engineering, Renewable Energy Laboratory, Jijel University, Old-Aissa P.O Box.98, Jijel, 18000, Algeria

ARTICLE INFO

Article history:
Received 4 January 2016
Received in revised form
24 February 2016
Accepted 6 March 2016

Keywords:
Neural network
Fuzzy logic
Controllers
Maximum power
Wind energy conversion system

ABSTRACT

This work presents a new control strategy to ensure maximum power point tracking for a DFIG (doubly fed induction generator) based WECS (wind energy conversion system). The proposed strategy uses neural networks and fuzzy logic controllers to control the power transfer between the machine and the grid using the indirect vector control and reactive power control techniques. This transfer is ensured by controlling the rotor via two identical converters. The first converter is connected to the RSC (rotor side) and the second is connected to the GSC (grid side) via a filter. The DC (Direct Current) link voltage is controlled by a fuzzy controller. This control strategy is used to control the rotor side currents and to protect the generator by limiting the output current (or voltage).

1. Introduction

In the area of wind power generation systems, where the wind speed varies considerably, VSG (variable speed generation) is more interesting than fixed speed systems [1,2]. In these systems, a MPPT (maximum power point tracking) adjusts a system quantity to maximize turbine power output [3,4]. The generator that operates at variable speeds is extremely attractive. So to exploit these advantages in wind power generation area, new control strategies should be designed, by taking into account all the parts of the system such as the grid, the structure complexity of the DFIG (doubly fed induction generator) with respect to the quality of the energy to be generated. In the absence of suitable control of the produced active and reactive powers many problems may appear when the generator is connected to the grid, such as, low power factor and harmonic pollution [4,5]. Several designs and arrangements have been investigated by using predictive functional and internal mode controllers, where satisfactory results in power response compared with those of the traditional methods, using a conventional PI (Proportional Integral) controller. However, these new methods are hard to implement, due to their complicated structures [6,7].

Among control objectives of WECSs (wind energy conversion system) much work has been achieved in the control of variable speed TSR (Time Speed Ratio) and/pitch controlled wind turbines with the main goal to bring them to the optimum operating point for maximum power conversion [3,6,8]. Many control schemes has been proposed for this purpose [9–13].

Adaptive control [14,15], which is a promising approach since it provides controllers the ability of learning and auto-adjustment as systems and/or environment change [16,17]. This feature is particularly useful for DFIGs which are immersed in highly stochastic and varying winds [18,19]. Different adaptive control schemes were proposed for achieving maximum power capture in WECSs in Ref. [20], the authors proposed an adaptive fuzzy control of a PMSG-based wind turbine, which dealt successfully with the uncertainties in the turbine parameters, in Ref. [21] an adaptive control scheme using radial basis function was proposed, in both works, a sliding supervisory term is introduced, this last can be a source of chattering and complexity, another limitation of this approach is the boundedness assumptions made on the control gain, its derivative and on the structural error [20], and the dynamics field vector [21].

* Corresponding author.
E-mail addresses: ahmed_medjber73@yahoo.fr (A. Medjber), belmilih@yahoo.fr (H. Belmili).

http://dx.doi.org/10.1016/j.energy.2016.03.026
0360-5442/

List of abbreviations

Ωt	Rotational speed of the turbine (m/s),
Ct	Turbine torque (N.m),
Ωmec	Mechanical speed of the turbine (m/s),
Cmec	Mechanical torque (N.m),
C_{em}	Electromagnetic torque (N.m),
C_{aero}	Aerodynamic torque (N.m),
Cp (λ,β)	power coefficient,
B	Orientation angle of the blades,
λ	Specific speed,
V_{wind}	Wind speed (m/s),
R	Ray of the blades (m),
f	Coefficient of friction (Ns/m),
J	Inertia (Kg/m^2),
G	Multiplier,
ρ	Air density (Kg/m^3),
V_{ds}, V_{qs}	Stator voltage direct (V),
I_{ds}, I_{qs}	Stator current direct (A),
V_{dr}, V_{qr}	Rotor voltage direct (V),
I_{dr}, I_{qr}	Rotor current Quadrature (A),
R_s, R_r	Resistance of stator and rotor (Ohm),
R_f	Filter resistance (Ohm).
V_g, I_g	Voltage and current side network (V), (A),
L_g	Inductance side network (H),
φ_{ds}, φ_{qs}	Stator flow direct (Weber),
φ_{dr}, φ_{qr}	Rotor flow Quadrature (Weber),
L_s,L_r	Stator and rotor inductance (H),
M	Mutual inductance (H),
ω_s, ω_r, ω_{gli}	Stator, rotor and slip angular speed (rd/s),
P	Number of the pair of the pole,
P_s, Q_s	Stator active and reactive power (Watt),
P_r, Q_r	Rotor active and reactive power (VAR),
P_g, Q_g	Active and reactive power side network (Watt), (VAR),

This paper is an alternative approach which has been proposed using optimized Neural Networks and Fuzzy Logic controllers to control the active and reactive powers through the rotor circuit, these types of controllers have been used due to their characteristics and benefits, such as their robustness, easy to understand and design, *via* the introduction of human expertise … etc [22–25].

The main objective of this work is to propose new neural network and adaptive fuzzy controller schemes for maximum wind power capture, applied to the doubly fed generator. The proposed schemes require controlling RSC (rotor side) and GSC (grid side). This paper is organized as follows. Section 1, briefly presents the model of the wind turbine, Section 2, presents a background of maximum power extraction objective. Section 3, presents modeling of asynchronous double feed Generator, the modeling of the indirect vector control power and the grid side converter, finalized by the DCLink voltages control. Section 5, outlines the proposed neural network and fuzzy logic controllers. Section 4, presents simulation results, Section 5 concludes the paper.

2. Wind turbine modeling

Fig. 1 represents the main parts of the studied WECS (wind energy conversion system).

The extracted power is expressed by: [26]

$$P_{\max} = \frac{1}{2} C_p(\lambda) \rho \pi R^2 V_{\text{wind}}^3 \tag{1}$$

$C_p(\lambda,\beta)$ is the power coefficient, expresses the aerodynamic efficiency of the turbine. With β is the pitch angle of the blades, so the ratio λ can be expressed as follows $\lambda = \frac{\Omega_t R}{V}$; C_P for 7.5 kW wind is defined as:

$$C_p(\lambda,\beta) = C_1\left(\frac{C_2}{\lambda_i} - C_3\beta - C_4\right)e^{\frac{C_5}{\lambda_i}} + C_6\lambda \tag{2}$$

With:

$$C_1 = 0.5176, C_2 = 116, C_3 = 0.4, C_4 = 5, C_5 = 21, C_6 = 0.0068 \tag{3}$$

$$\frac{1}{\lambda_i} = \frac{1}{\lambda + 0.008\beta} - \frac{0,035}{\beta^3 + 1}$$

The limit of Betz is defined by $C_p = 0.48$ for a specific speed $\lambda_{opt} = 8.1$ the WECS provides optimal power rating to determine the evolution of the mechanical speed from the total torque C_{mec}

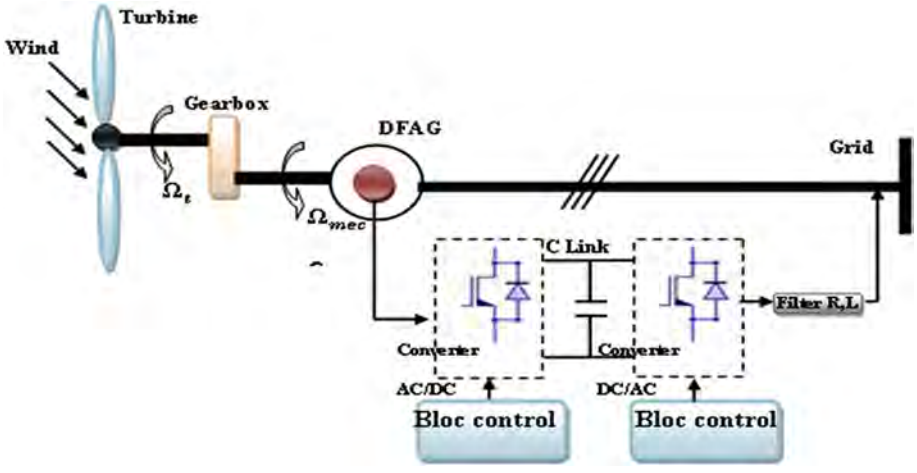

Fig. 1. The studied wind energy conversion system.

applied to the rotor of the DFAM (Double Fed Asynchrone Machine) we apply the fundamental equation of dynamics:

$$J\frac{d\Omega_{mec}}{dt} = C_{aero} - C_{mec} - f\Omega_{mec} \tag{4}$$

The previous equations used to establish the block diagram of the model of the turbine, Fig. 2.

3. Maximum power point tracking

The maximum power from wind energy, for $\lambda_{opt} = 0.81, \beta = 0$ that gives $C_p = 0.47$, that allows adjusting the torque of the turbine, so as to set its speed to its reference is written by: $\Omega_{tref} = \frac{\lambda_{opt} V_{wind}}{R}$, it is very important to note that the turbine is to be used in the three zones of operation, Fig. 3. Zone I when the wind speed is less than a cut in speed, the turbine is stopped. Zone II, in this zone, the power is proportional to the cube of the wind speed. Zone III as from the rated speed, once the maximum speed reached it is dangerous to let the WECS turn [3–5] mechanical braking systems, often a disc brake are active to completely stop the turbine. To ensure maximum turbine efficiency and maintain the coefficient power at its maximum [8,9,17,23].

4. Modeling double feed induction generator DFIG

Electrical equations of DFIG can be written [26,27]:

$$\begin{cases} V_{ds} = R_s I_{ds} + \dfrac{d\varphi_{ds}}{dt} - \omega_s \varphi_{qs} \\ V_{qs} = R_s I_{qs} + \dfrac{d\varphi_{qs}}{dt} + \omega_s \varphi_{ds} \\ V_{dr} = R_r I_{dr} + \dfrac{\varphi_{dr}}{dt} - \omega_{sli} \varphi_{qr} \\ V_{qr} = R_r I_{qr} + \dfrac{d\varphi_{qr}}{dt} + \omega_{gli} \varphi_{dr} \end{cases} \tag{5}$$

$$\text{With : } \omega_{sli} = \omega_s - P\Omega_{mec} \tag{6}$$

p: Number of the pole pairs,

$$\begin{cases} \varphi_{ds} = L_s I_{ds} + M I_{dr} \\ \varphi_{qs} = L_s I_{qs} + M I_{qr} \\ \varphi_{dr} = L_r I_{dr} + M I_{ds} \\ \varphi_{qr} = L_r I_{qr} + M I_{qs} \end{cases} \tag{7}$$

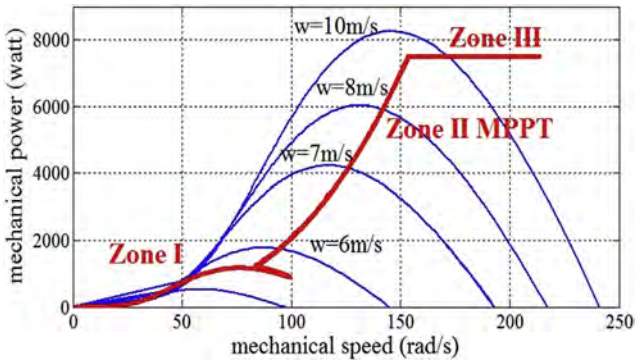

Fig. 3. Typical curve of the extracted power according to the wind speed.

$$C_{em} = \frac{3PM}{2}(\varphi_{ds} I_{qr} - \varphi_{qs} I_{dr}) \tag{8}$$

C_{em}:Electromagnetic torque,

The active and reactive powers of the DFIG stator and rotor are written as:

$$\begin{cases} P_s = V_{ds} I_{ds} + V_{qs} I_{qs} \\ Q_s = V_{qs} I_{ds} - V_{ds} I_{qs} \\ P_r = V_{dr} I_{dr} + V_{qr} I_{qr} \\ Q_r = V_{qr} I_{dr} - V_{dr} I_{qr} \end{cases} \tag{9}$$

4.1. Indirect vector control of the DFIG power

Consider that the voltage and frequency are constant, from Equation (8), the electromagnetic torque is strongly coupled to the flows and currents, which makes the control of the DFIG very difficult. In order to simplify the task, the model is approximated to the DC machine, which has the advantage of having a natural coupling between flows and currents. For this, applying control vector; and choosing a two-phase dq (direct-quadrature) axis reference frame connected to the rotating field. Stator flux φ_s is oriented along the axis. Thus, it can be written as [27],

$$\varphi_{qs} = 0, \varphi_{ds} = \varphi_s \tag{10}$$

For medium and high power machine, the stator resistance can be neglected [11], hence:

$$\begin{cases} V_{ds} = 0 \\ V_{qs} = V_s = \omega_s \varphi_s \end{cases} \tag{11}$$

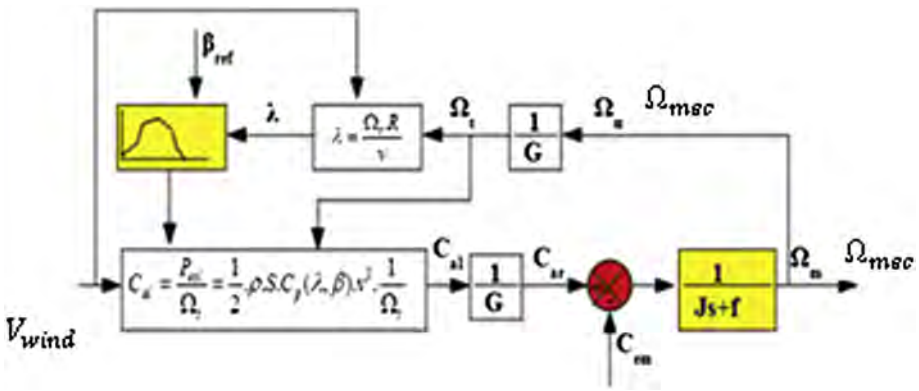

Fig. 2. Bloc diagram of the turbine.

$$\begin{cases} P_s = -V_s \dfrac{M}{L_s} I_{qr} \\ Q_s = V_s \dfrac{\varphi_s}{L_s} - V_s \dfrac{M}{L_s} I_{dr} \end{cases} \quad (12)$$

$$\begin{cases} P_r = g \dfrac{MV_s}{L_S} I_{qr} \\ Q_r = g \dfrac{MV_s}{L_s} I_{dr} \end{cases} \quad (13)$$

$$\begin{cases} P_t = P_s + P_r = (g-1) \dfrac{MVs}{L_s} I_{qr} \\ Q_t = Q_s + Q_r = \dfrac{V_s^2}{\omega_s L_s}. + (g-1) \dfrac{MV_s}{L_s} I_{dr} \end{cases} \quad (14)$$

According to Equation (8), the electromagnetic torque is described by the following equation [29]:

$$C_{em} = \frac{3}{2} \frac{PM}{L_s} \varphi_{ds} I_{qr}, \text{ then, } I_{qref} = \frac{2}{3} \frac{L_s \omega_s}{PMV_s} C_{emref} \quad (15)$$

Following Equation (13), the reactive power of the stator can be controlled by a direct rotor current I_{dr} with the aim to have a unit stator side power factor, maintaining the stator reactive power zero, and the reference current becomes:

$$I_{dref} = \frac{V_s}{M\omega_S} \quad (16)$$

The rotor side converter control system is illustrated in Fig. 4.

4.2. Modeling of the GSC (grid side converter)

The role of RL (Resistor–Inductor) filter is to keep the DClink voltage constant with a current and the power factor side network as unit. According to Fig. 5, the three-phase voltages can be expressed as follows [28,29]:

$$\begin{cases} V_{g1} = -R_f i_{g1} - L_g \dfrac{di_{g1}}{dt} + V_{s1} \\ V_{g2} = -R_f i g_2 - L_g \dfrac{di_{g2}}{dt} + V_{s2} \\ V_{g3} = -R_f i_{g3} - L_g \dfrac{di_{g3}}{dt} + V_{s3} \end{cases} \quad (17)$$

Using the park transformation, Equation (17) can be expressed as follows:

$$\begin{cases} V_{gd} = -R_f i_{gd} - L_g \dfrac{di_{gd}}{dt} + L_g \omega_s i_{gq} \\ Vgq = -R_f i_{gq} - L_g \dfrac{di_{gq}}{dt} - L_g \omega_s i_{gd} + V_{qs} \end{cases} \quad (18)$$

The coupling voltages are written as follows:

$$\begin{cases} e_{gd} = L_g \omega_s i_{gq} \\ e_{gq} = -L_g \omega_s i_{gd} + V_{qs} \end{cases} \quad (19)$$

Thus the expressions of active and reactive power are expressed respectively by the following equations:

$$\begin{cases} P_g = V_{ds} i_{gd} + V_{qs} i_{gq} \\ Q_g = V_{qs} i_{gd} - V_{ds} i_{gq} \end{cases} \quad (20)$$

According of previous hypotheses ($V_{ds} = 0$), Equation (20) can be written as:

$$\begin{cases} P_g = V_s i_{gq} \\ Q_g = V_s i_{gd} \end{cases} \quad (21)$$

Losses in the converter were considered as nonexistent i.e.: $i_g = i_{red} = i_{gq}$ then the powers of DC link bus are defined as follows:

$$\begin{cases} P_g = V_{dc} i_{gq} \\ P_c V_{dc} i_c \\ P_{ond} = V_{dc} i_{ond} \\ P_g = P_{red} = P_c + P_{ond} \end{cases} \quad (22)$$

The synoptic diagram of the grid side subsystem in the referential dq stator rotating field shows that currents control can be

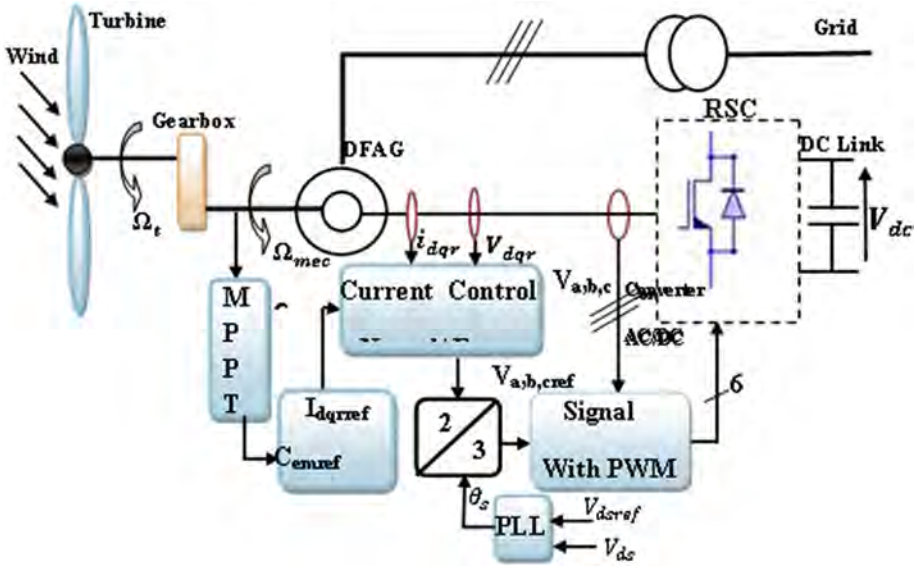

Fig. 4. Diagram control of the RSC.

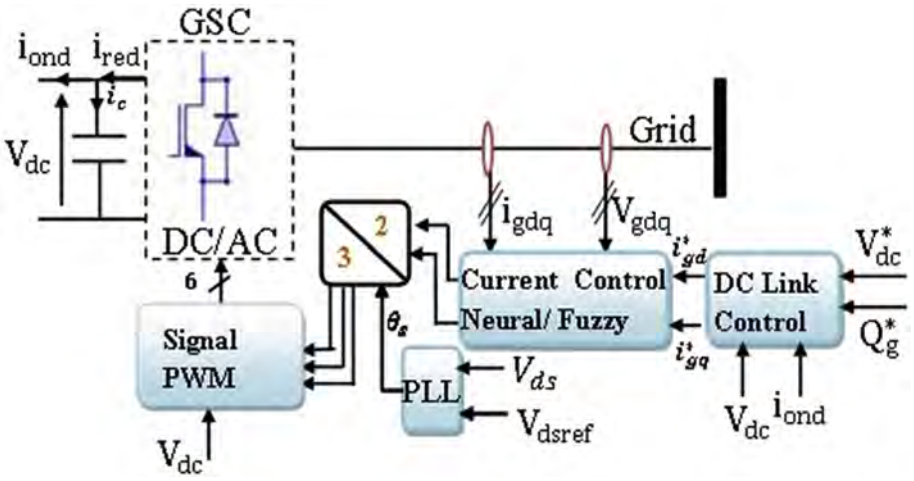

Fig. 5. Scheme of the grid side converter control.

established according to the given filter R_g, L_g [6,28]. Such, each axis can be controlled independently. The current control schema is given in Fig. 6; this control block includes the references currents direct and quadrature in input, the coupling block and the compensation term. The controllers used are types neural network and fuzzy logic. The direct current component is used to control the reactive power network side. The quadrature component, in turn, is used to adjust the DC link voltage. The block diagram in the grid side is [8,29].

4.3. DC-link voltages control

Fig. 7 shows the block diagram of the DC link voltage control scheme. For maintaining a constant voltage [8,30] with a neural network and fuzzy controllers generating the reference current in the capacitor.

5. Neural network and fuzzy logic controllers

5.1. Neural network controller design

The idea is to substitute the fuzzy controller (rotor side and grid side) by neural network regulator, for this, a graphic interface based on NNFTool (Neural Network Fitting Tool) in Matlab software tool is used for the learning, via Levenberg–Marquardt propagation algorithm. This step is a back propagation of the error of the output layer to the input layer. It can be done by modifying and adapting the weights of NN (Neural Network) to converge to the optimum values and constants (the learning coefficient must be 0.93 or greater). The problem is to find a structure (number of hidden layers and number of neurons in each hidden layer), which gives better results. For this, purpose several tests to determine the optimal network architecture have been carried. The most efficient choice was to take a neural network structure in an input layer to a neuron, a single hidden layer with three neurons and an output layer neuron like it shows in Fig. 8. The activation used the sigmoid function [3,21].

$$X^{(1)}(k) = \left[w^{(1)}(k)\right]^T . X(k) \tag{23}$$

$$O^{(1)}(k) = f^{(1)}\left(X^{(1)}(k)\right) \tag{24}$$

$$X^{(2)}(k) = \left[w^{(2)}(k)\right]^T O^{(1)}(k) \tag{25}$$

$$O^{(2)}(k) = f^{(2)}\left(X^{(2)}(k)\right) \tag{26}$$

$$Y(k) = O^{(2)}(k) \tag{27}$$

X (k) is the input vector of dimension (m = 1).

$W^{(1)}(k)$, $W^{(2)}(k)$ are respectively the matrix of the weight in hidden layer and output layer size (m × n) = (1 × 3) and (n × p) = (3 × 1).

$X^{(1)}(k)$,$O^{(1)}(k)$ $X^{(2)}(k)$,$O^{(2)}(k)$ are respectively the input and the output vectors of the hidden layer, the output layer size (n × 1) = (3 × 1) and (p × 1) = (1 × 1).

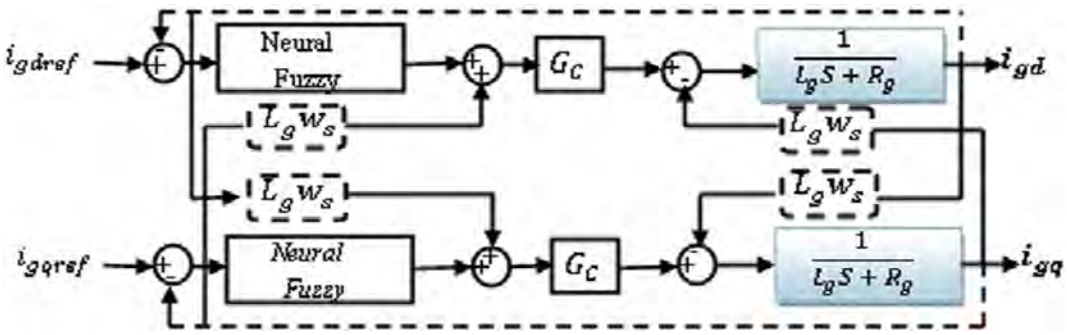

Fig. 6. Control loop of the currents filter.

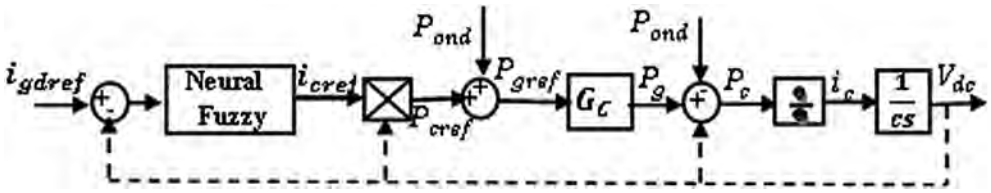

Fig. 7. Control loop of the DClink voltage.

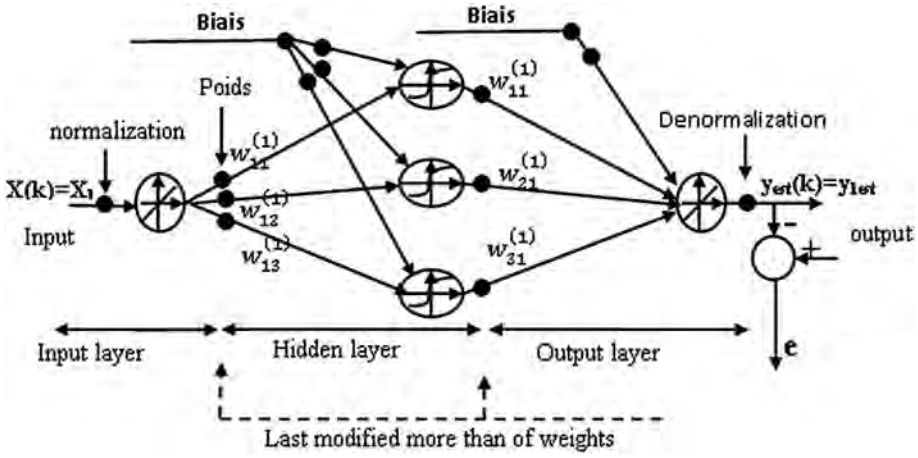

Fig. 8. Structure of neural networks with a single hidden layer.

$\Lambda^{(1)}(k)$ $\Lambda^{(2)}(k)$ are the back propagation error vectors of the hidden layer and the output size $(n \times 1) = (3 \times 1)$ and $(p \times 1) = (1 \times 1)$. $f^{(1)}(.)$,$f^{(2)}(.)$ are respectively the activation functions of the hidden layer and the output layer (this latter is an identity function). From these equations, the output Y (k) can be calculated to show the neural network in the Fig. 8 as follows:

$$Y(k) = \left[w^{(2)}(k)\right]^T f^{(1)}\left(\left[w^{(1)}(k)\right]^T\right)^T .X(k)\Big) \tag{28}$$

The weights of the output layer are updated as follows:

$$\Delta w^{(2)}(k) = -\sigma O^{(1)}(k)\left(\Lambda^{(2)}(k)\right)^T \tag{29}$$

With:

$$\Lambda^{(2)}(k) = Y(k) - Y_{est}(k)$$

The weights of the hidden layer are calculated as follows:

$$\Delta w^{(1)}(k) = -\sigma.X(k).\left(\Lambda^{(1)}(k)\right)^T \tag{30}$$

Hence:

$$X^{(1)}(k) = O_i^{(1)}.\left(1 - O_i^{(k)}\right).\sum_{j=1}^{p} w_{ij}(k)\Lambda_j^{(2)}(k), i = 1, 2, \ldots\ldots\ldots, n \tag{31}$$

5.2. Fuzzy logic controller design

The aim is to control the DFIG and grid power. The developed controller uses the scheme proposed by Mamdani [32], Fig. 9.

The major problem encountered during the synthesis of the fuzzy controller is the choice of adaptation parameters that plays an important role in assuring the best performance [19,20,23,33]. So, parameters are varied until it can be a transient phenomenon proper setting [31]. The selected triangular membership functions are presented on Fig. 10. Such, (a) error for input, (b) error variation, and (c) function for output and Table 1 which presents the Decision rules.

6. Simulation results of both fuzzy logic and neuron network controllers

Mathematical model are implemented under MATLAB/Simulink, by using variable wind profile (Fig. 11) applied to the DFIG for a period of 15 s, in order to have an active power reference. Reference power reactive is maintained zero (i.e. maintain a unity power factor stator side).

6.1. Results interpretation

Figures above shows the performance of neural network-fuzzy logic controllers and vector control in stator active and reactive power applied to the DFIG based WECS. The mechanical speed of the rotor follows the evolution of wind speed which varies between 100rd/s et 200rd/s which corresponds to the variation of wind between 6.5 m/s and 13.7 m/s respectively.

The reference magnitudes for the active and reactive power are attended by DFIG by using fuzzy logic and neural network controllers in Figs. 12 and 13respectively. The active power is negative,

Fig. 9. Structure of a fuzzy logic controller. Ge, dGe and Gu are the adaptation parameters of fuzzy controller.

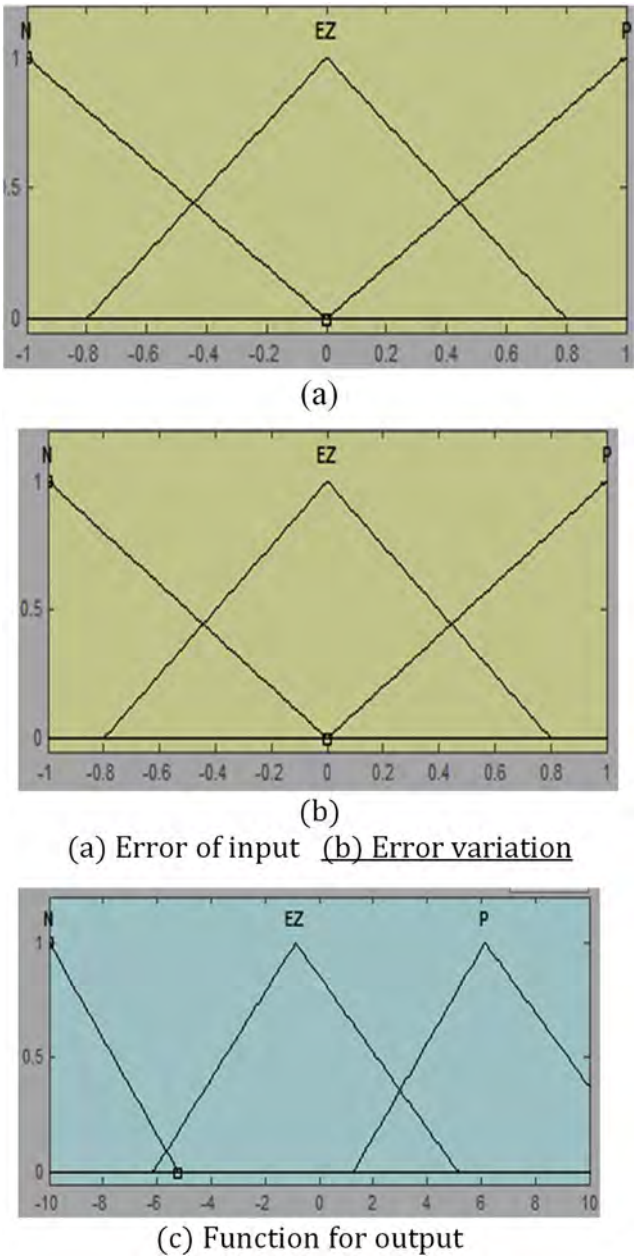

Fig. 10. Memberships functions of a fuzzy logic controller.

which means that the DFIG operates as generators. However, the stator reactive power is set to zero in order to have a factor power as unit; this is observed on the shape of the stator current which is in phase opposition with the voltage (see Figs 14–19). This shows that the active power of the generator is sent to the network.

Figs. 20 and 21 represent the regulation of the DC bus voltage around a Vdc = 620 V which is the reference. It presents some

Table 1
Decision rules.

U		e		
		N	EZ	P
de/dt	N	N	P	P
	EZ	N	P	P
	P	N	P	P

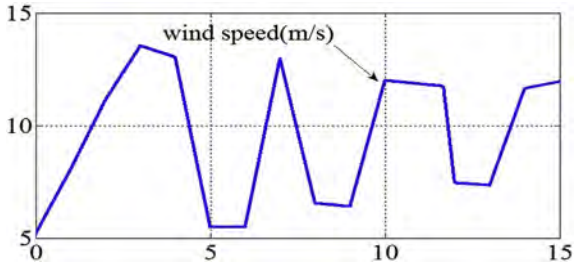

Fig. 11. Wind speed profile applied to the wind turbine.

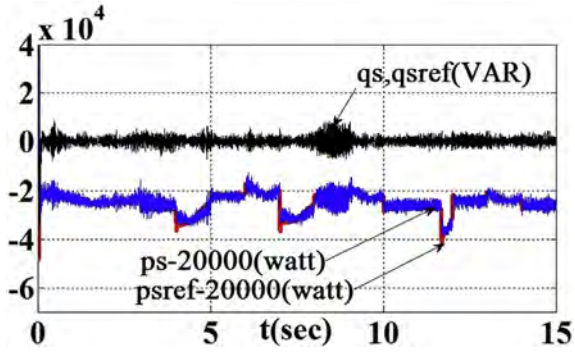

Fig. 12. Active and reactive power of DFIG by using fuzzy logic controller.

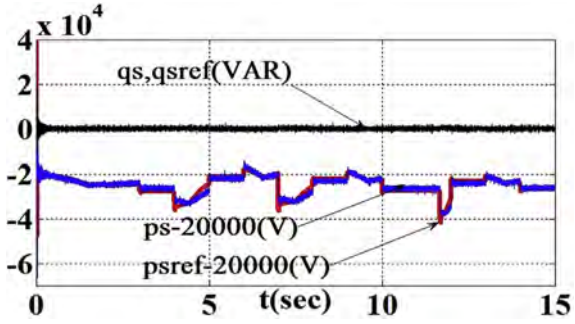

Fig. 13. Active and reactive power of DFIG by using of neural network controller.

disturbances, this is due to the fact that the DC link voltage rises or falls with an increase or decrease of the exploitation of the electric power.

In order to regulate the V_{dc} voltage, the inverter intervenes by injecting the surplus of power to the grid and vice versa, to discharge/charge the capacitor until ($V_{dc} = V_{dc\_ref}$), at same time,

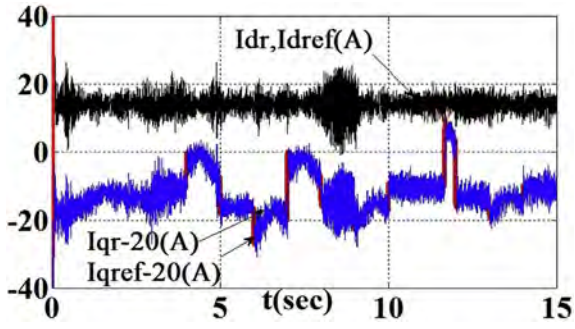

Fig. 14. Direct and quadrature currents by using fuzzy logic controller.

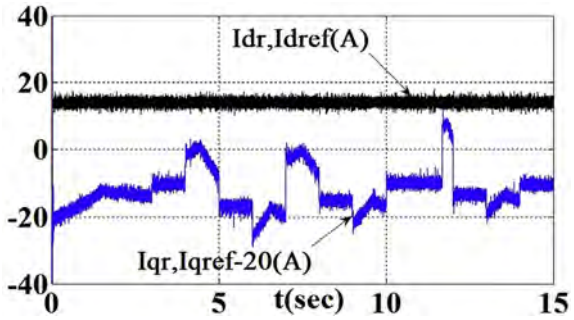

Fig. 15. Direct and quadrature currents by using neural network controller.

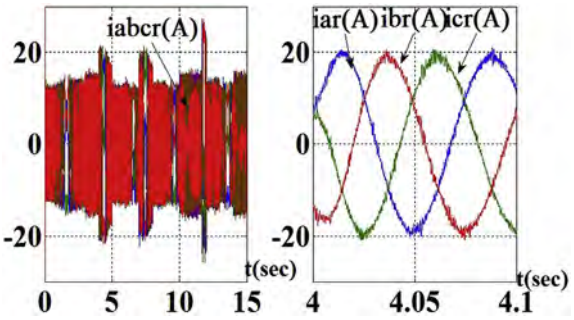

Fig. 16. Phase rotor currents by using fuzzy logic controller.

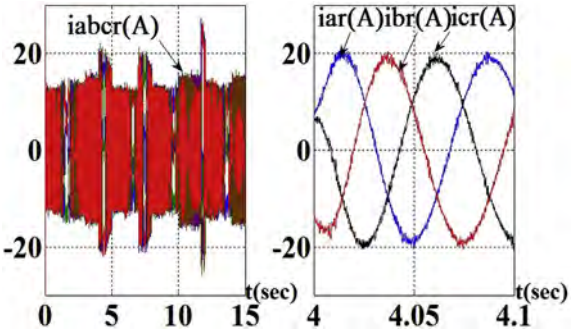

Fig. 17. Phase rotor currents by using neural network controller.

the inverter assures transfer of the exploited power to the grid (the active and reactive power are injected to the grid) see Figs. 22–27.

From the simulation results, it can be concluded that the response time obtained by the Neuron controller is considerably reduced, the peak values are exceeded and limited compared to those of the fuzzy logic controller (see Figs. 28 and 29).

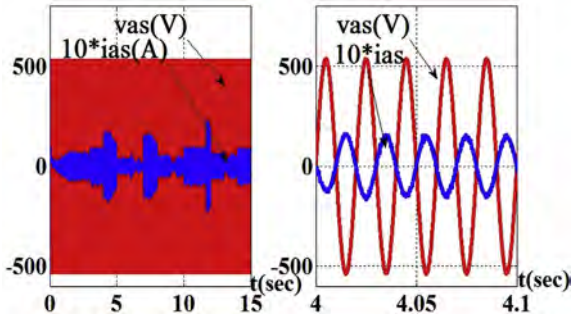

Fig. 18. Grid voltage and the phase stator currents by using fuzzy logic controller.

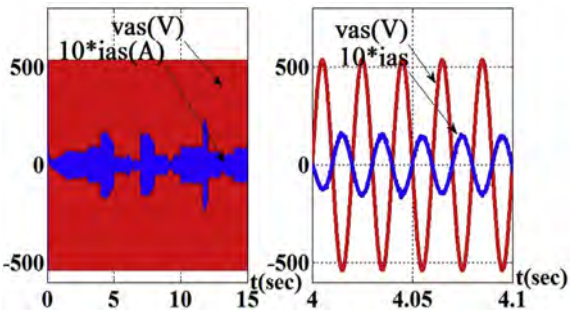

Fig. 19. Grid voltage and the phase stator currents by using neural network controller.

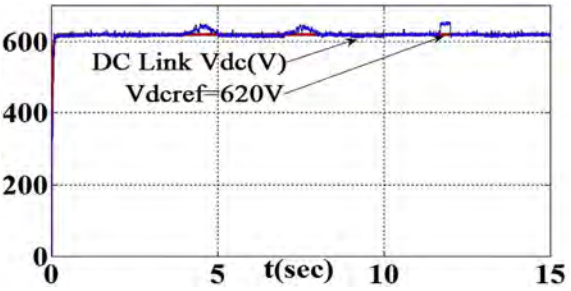

Fig. 20. DCLink voltage by using fuzzy logic controller.

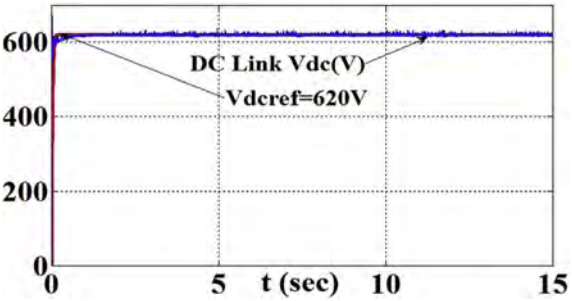

Fig. 21. DCLink voltage by using neural network controller.

7. Conclusions

The main contribution of this work is the introduction of new control technique using neural networks and fuzzy logic controllers applied to grid connected DFIG based WECS. For this, the vector

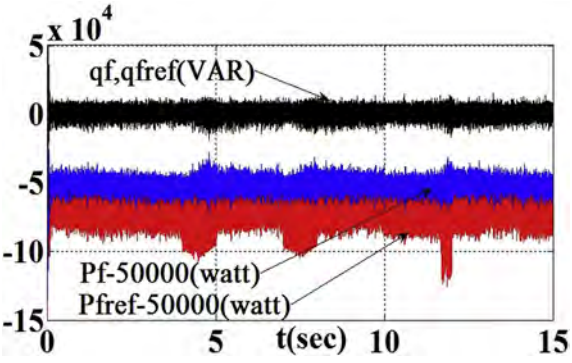

Fig. 22. Active and reactive power of the grid side converter by using fuzzy logic controller.

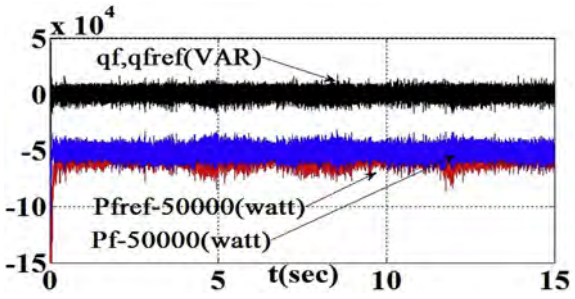

Fig. 23. Active and reactive power of the grid side converter by using neural network controller.

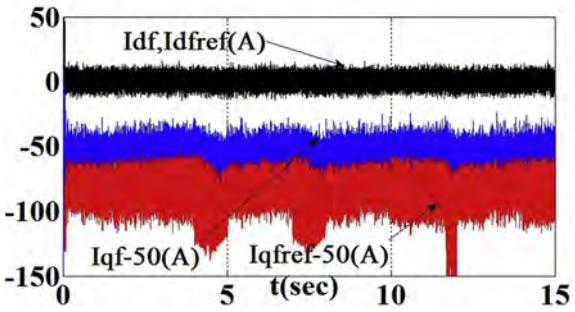

Fig. 24. Direct current and quadrature of the rotor side converter by using fuzzy logic controller.

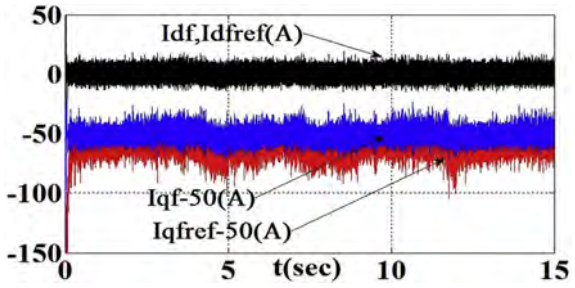

Fig. 25. Direct current and quadrature of the grid side converter by using neural network controller.

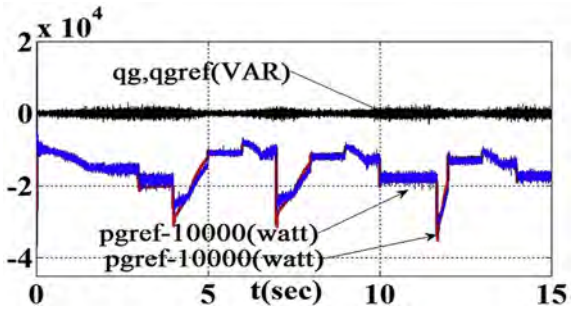

Fig. 27. Active and reactive power of the grid by using neural network controller.

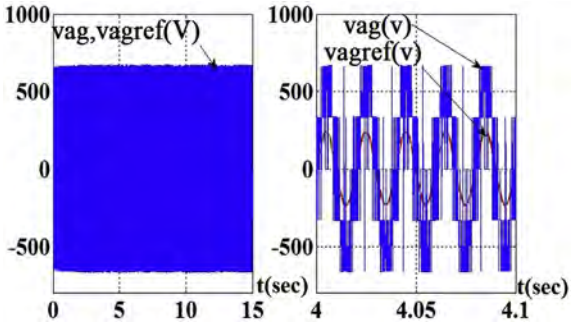

Fig. 28. Output voltage of the grid side converter by using fuzzy logic controller.

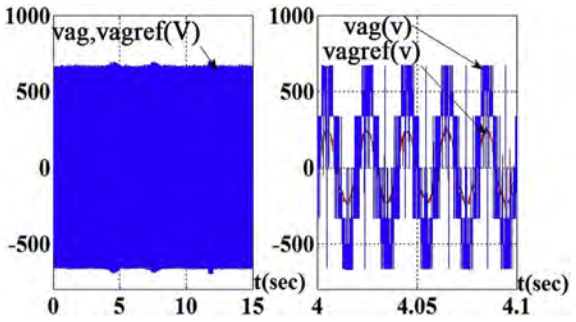

Fig. 29. Output voltage of the grid side converter by using neural network controller.

control is established via an electronic converter and a PWM (Pulse-Width Modulation) based switching. This electric combination allows the WECS control strategy for the maximum power point extraction application using a fuzzy control of the speed variation. Afterward, the extracted electrical power is injected to the grid via a three-phase voltage inverter, and the DC link voltage is regulated. The analysis of the obtained results shows clearly an acceptable degree of effective regulation by the proposed controllers. It can be seen that after a change in wind speed, the measured powers follow the change of the reference. These results demonstrated that the proposed structure based on optimized neural network and fuzzy logic controllers may consider as an interesting solution in the wind energy conversion systems using a DFIG wind turbine.

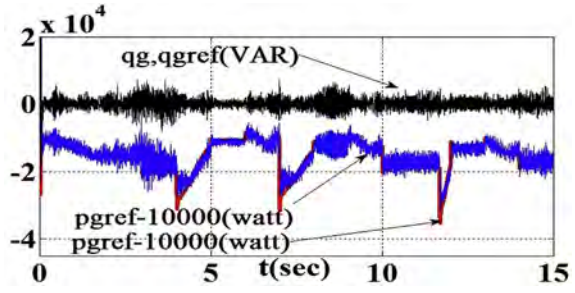

Fig. 26. Active and reactive power of the grid by using fuzzy logic controller.

References

[1] Ackermann T. Wind power in power Systems. John Wiley and Sons; 2005.
[2] Wind force 12. October 2002. Report by the European Wind Energy Association (EWEA).
[3] Lin Whei-Min, Hong Chih-Ming, Cheng Fu-Sheng. Fuzzy neural network output maximization control for sensor less wind energy conversion system. Energy 2010;35:592–601.
[4] Yin Xiu-xing, Lin Yong-gang, Li Wei, Gu Ya-jing, Lei Peng-fei, Liu Hong-wei. Sliding mode voltage control strategy for capturing maximum wind energy based on fuzzy logic control. Electr Power Energy Syst 2015;70:45–51. Elsevier.
[5] Suganthi L, Iniyan S, Samuel Anand A. Applications of fuzzy logic in renewable energy systems. Renew Sustain Energy Rev 2015;48:585–607.

[6] Ourici A. Power control in a doubly fed induction machine. World Acad Sci Eng Technol 2011;77(53):51–4.
[7] Reznik Leonid. Fuzzy controllers. Melbourne, Australia: Newnes Publisher. Victoria University of Technology; 1997.
[8] Petković Dalibor, Ćojbašić Žarko, Nikolić Vlastimir, Shamshirband Shahaboddin, Kiah Miss Laiha Mat, Anuar Nor Badrul, et al. Adaptive neuro-fuzzy maximal power extraction of wind turbine with continuously variable transmission. Energy January 2014;64:868–74.
[9] Belmokhtar K, Doumbia M, Agbossou K. Novel fuzzy logic based sensorless maximum power point tracking strategy for wind turbine systems driven DFIG (doubly-fed induction generator). Energy 2014;76:679–93. Elsevier.
[10] Petković Dalibor, Shamshirband Shahaboddin, Anuar Nor Badrul, Naji Sareh, Kiah Miss Laiha Mat, Gani Abdullah. Adaptive neuro-fuzzy evaluation of wind farm power production as function of wind speed and direction. Stoch Environ Res Risk Assess March 2015;29(3):793–802. http://dx.doi.org/10.1007/s00477-014-0901-8.
[11] Petković Dalibor, Shamshirband Shahaboddin, Ćojbašić Žarko, Nikolić Vlastimir, Anuar Nor Badrul, Sabri Aznul Qalid Md, et al. Adaptive neuro-fuzzy estimation of building augmentation of wind turbine power. Comput Fluids 25 June 2014;97:188–94.
[12] Petković Dalibor, Shamshirband Shahaboddin, Anuar Nor Badrul, Saboohi Hadi, Abdul Wahab Ainuddin Wahid, Protić Milan, et al. An appraisal of wind speed distribution prediction by soft computing methodologies: a comparative study. Energy Convers Manag August 2014;84:133–9.
[13] Petković Dalibor, Ab Hamid Siti Hafizah, Ćojbašić Žarko, Pavlovic Nenad T. Adapting project management method and ANFIS strategy for variables selection and analyzing wind turbine wake effect. Nat Hazards November 2014;74(2):463–75. http://dx.doi.org/10.1007/s11069-014-1189-1.
[14] Petković Dalibor, Ćojbašić Žarko, Nikolić Vlastimir. Adaptive neuro-fuzzy approach for wind turbine power coefficient estimation. Renew Sustain Energy Rev December 2013;28:191–5.
[15] Gani Abdullah, Mohammadi Kasra, Shamshirband Shahaboddin, Altameem Torki A, Petković Dalibor, Sudheer Ch. A combined method to estimate wind speed distribution based on integrating the support vector machine with firefly algorithm. Environ Prog Sustain Energy October 2015;00:1–9. http://dx.doi.org/10.1002/ep.12262.
[16] Petković Dalibor, Shamshirband Shahaboddin. Soft methodology selection of wind turbine parameters to large affect wind energy conversion. Electr Power Energy Syst November 2015;69:98–103. http://dx.doi.org/10.1016/j.ijepes.2014.12.086.
[17] Nikolić Vlastimir, Shamshirband Shahaboddin, Petković Dalibor, Mohammadi Kasra, Ćojbašić Žarko, Altameem Torki A, et al. Wind wake influence estimation on energy production of wind farm by adaptive neuro-fuzzy methodology. Energy February 2015;80:361–72. http://dx.doi.org/10.1016/j.energy.2014.11.078.
[18] Petković Dalibor. Adaptive neuro-fuzzy approach for estimation of wind speed distribution. Electr Power Energy Syst December 2015;73:389–92. http://dx.doi.org/10.1016/j.ijepes.2015.05.039.
[19] Kairousa D, Wamkeueb R. DFIG-based fuzzy sliding-mode control of WECS with a flywheel energy storage. Elsevier Electr Power Syst Res 2012;93:16–23.
[20] Nguyen HM, Naidu DS. Direct fuzzy adaptive control for standalone wind energy conversion systems. In: Proceedings of the world congress on engineering and computer science, vol II; 2012. p. 994–9. San Fransisco, USA.
[21] Mayosky MA, Cancelo GIE. Direct adaptive control of wind energy conversion systems using Gaussian networks. IEEE Trans Neural Netw 1999;10(4).
[22] Petković Dalibor. Adaptive neuro-fuzzy optimization of the net present value and internal rate of return of a wind farm project under wake effect. JCC Bus Econ Res J March 2015;8:11–28. http://dx.doi.org/10.7835/jcc-berj-2015-0102.
[23] Nikolić Vlastimir, Petković Dalibor, Shamshirband Shahaboddin, Ćojbašić Žarko. Adaptive neuro-fuzzy estimation of diffuser effects on wind turbine performance. Energy October 2015;89:324–33. http://dx.doi.org/10.1016/j.energy.2015.05.126.
[24] Nikolić Vlastimir, Petković Dalibor, Por Lip Yee, Shamshirband Shahaboddin, Zamani Mazdak, Ćojbašić Žarko, et al. Potential of neuro-fuzzy methodology to estimate noise level of wind turbines. Mech Syst Signal Process January 2016;66–78:715–22. http://dx.doi.org/10.1016/j.ymssp.2015.03.013.
[25] Ali Abdulrahim Haroun, Shamshirband Shahaboddin, Anuar Nor Badrul, Petković Dalibor. DFCL: Dynamic fuzzy logic controller for intrusion detection. FACTA Univ Ser Mech Eng August 2014;12(2):183–93. ISSN 2335-0164.
[26] Zhen S, Hongyu W, Ying L. Modeling and simulation of doubly-fed induction wind power system based on Matlab/Simulink. Chinese, ISBN: 978-1-4673-5533-9. In: IEEE. Control and decision Conference (CCDC), 2013; 2013. p. 4070–5. http://dx.doi.org/10.1109/CCDC. 6561663.
[27] EL-helw H, Tennakoon Sarath B. Vector control of a doubly fed induction generator for standalone wind energy application. ISBN: 978-9-0758-1512-2. In: IEEE, published in wind power to the grid, conference Delft 2008; 2008. p. 1–6. http://dx.doi.org/10.1109/EPEWECS. 4497318.
[28] Yufei T, Haibo H, Zhen N, Jinyu W, Xianchao S. Reactive power control of grid-connected wind farm based on adaptive dynamic programming. Elsevier Neuro Comput 2014;125:125–33.
[29] Sushanta Kumar S, Ashish Kumar S. Modeling and simulation of AC/DC grid side voltage source converter used in wind power generation system. In: IEEE. 2014 International Conference on circuit, power and computing technologies [ICCPCT]; 2014. p. 484–9. http://dx.doi.org/10.1109/ICCPCT. 7054909.
[30] Shuhui L, Ling X. PWM converter control for grid integration of wind turbines with enhanced power quality. In: IEEE. Industrial electronics, 34th Annual Conference 2008; 2008. p. 2218–24. http://dx.doi.org/10.1109/IECON.475830.
[31] Whei-Min L, Chih-Ming H, Fu-Sheng C. Fuzzy neural network output maximization control for sensor less wind energy conversion system. Elsevier. Energy 2010;35:592–601.
[32] Mamdani EH. Advances in the linguistic synthesis of fuzzy controllers. Int J Man-Machine Stud November 1976;8(6):669–78.
[33] Shahaboddin Shamshirband. Generalized adaptive neuro-fuzzy based method for wind speed distribution prediction. Flow Meas Instrum June 2015;43:47–52. http://dx.doi.org/10.1016/j.flowmeasinst.2015.03.003.